Received 10 November 2014; revised 5 April 2015 and 2 May 2015; accepted 14 May 2015. Date of publication 20 May 2015; date of current version 19 June 2015. The review of this paper was arranged by Editor T.-L. Ren.

Digital Object Identifier 10.1109/JEDS.2015.2435492

Ferroelectricity of $HfZrO_2$ in Energy Landscape With Surface Potential Gain for Low-Power Steep-Slope Transistors

MIN HUNG LEE[1] (Member, IEEE), Y.-T. WEI[1], C. LIU[1], J.-J. HUANG[2], MING TANG[3], YU-LUN CHUEH[4], K.-Y. CHU[1], MIIN-JANG CHEN[2], HENG-YUAN LEE[5], YU-SHENG CHEN[5], LI-HENG LEE[5], AND MING-JINN TSAI[5]

1 Institute of Electro-Optical Science and Technology, National Taiwan Normal University, Taipei 11677, Taiwan
2 Department of Material Science and Engineering, National Taiwan University, Taipei 10617, Taiwan
3 Device Design Division, PTEK Technology Company Ltd., Hsinchu 30059, Taiwan
4 Department of Materials Science and Engineering, National Tsing Hua University, Hsinchu 30013, Taiwan
5 Electronics and Optoelectronics Research Laboratories, Industrial Technology Research Institute, Hsinchu 31040, Taiwan

CORRESPONDING AUTHOR: M. H. LEE (e-mail: mhlee@ntnu.edu.tw)

This work was supported in part by the National Science Council under Grant 102-2221-E-003-030-MY3, Grant 103-2221-E-003-023, and Grant 103-2622-E-002-031, in part by the National Nano Device Laboratories, and in part by the National Center for High-Performance Computing, Taiwan.

ABSTRACT The corresponding energy landscape and surface potential are deduced from the experimental ferroelectricity of $HfZrO_2$ (HZO) for low-power steep-slope transistor applications. The anti-ferroelectric (AFE) in annealed 600°C HZO extracted electrostatic potential gain from the measured polarization hysteresis loop and calculated subthreshold swing 33 mV/dec over six decades of I_{DS}. A feasible concept of coupling the AFE HZO is experimentally established with the validity of negative capacitance and beneficial for steep-slope FET development in future generation.

INDEX TERMS Ferroelectric (FE), subthreshold swing (SS), negative capacitance (NC).

I. INTRODUCTION

Integrated ferroelectric (FE) hafnium-based field-effect transistors (FETs) as dielectric with negative capacitance (NC) effect is compatible with CMOS process and provides a feasible and synergistic concept. For NC-FETs, the polymer FE was studied and integrated for a < 60 mV/decade swing [1], [2]. BTO ($BaTiO_3$) and PZT ($PbZrTiO_3$) were used for demonstrating steep-slope MOSFET and TFET [3], [4]. To benefit scaling down and process compatibility, the monoclinic HfO_2 with suitable dopants for FE transition attracted lots of attention, such as tetragonal ZrO_2 [5]–[7], cubic Y:HfO_2 [8], tetragonal Si:HfO_2 [9], and tetragonal Al:HfO_2 [10]. The traces of dopants made the precise control difficult except ZrO_2:HfO_2, which was a nearly equal mixture of ZrO_2 and HfO_2 [5]–[7]. To accomplish NC effect for steep-slope FET (SS-FET), the antiferroelectric (AFE) characteristics for gate stack were required [3].

In this work, the $HfZrO_2$ (HZO) was deposited and deduced the corresponding energy landscape from the ferroelectricity to understand the surface electrostatic potential of FET with subthreshold operation. The feasible concept of coupling the AFE polarization HZO was applied, which were experimentally established with the validity of the negative capacitance concept.

II. EXPERIMENTAL

A standard 6-inch MOS (metal-oxide-semiconductor) based line was employed in this study. First, a 200-nm-thick TiN was deposited on the Si substrate by sputtering. Thin films of HZO were grown by remote plasma atomic layer deposition on TiN/Si substrate. The HZO films with a Hf:Zr ratio of 0.5:0.5 consisted of one cycle of HfO_2 and one cycle of ZrO_2. The thickness of HZO films was controlled by about 9.5 nm, as confirmed by the spectroscopic ellipsometry at $\lambda = 633$ nm and HR-TEM (high-resolution transmission electron microscopy) as shown in Fig. 1(a). Then, the 40-nm-thick TiN was covered on the prior insulator layer by a sputtering system sequentially. The diode area was then defined by photolithography and etched by RIE to form the

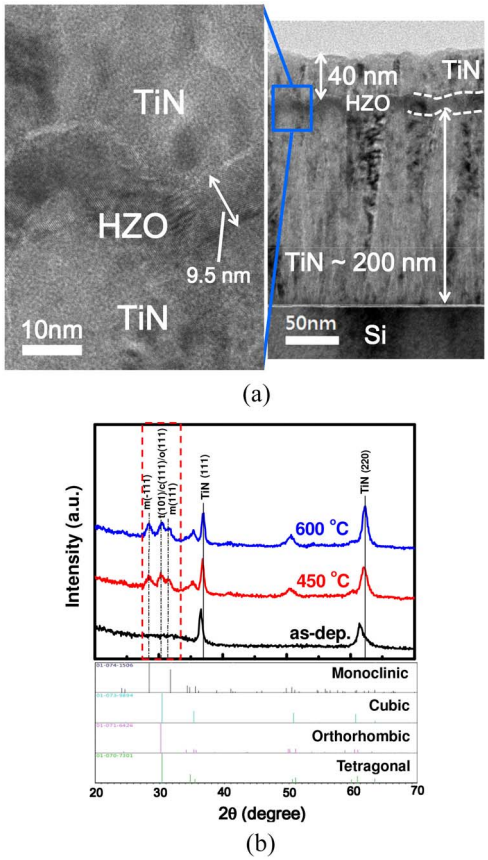

FIGURE 1. (a) Cross-sectional TEM of TiN/HZO/TiN. The HZO thickness ~9.5 nm and the lattice image are observed. Note that the PVD TiN leads interface rough due to column structure. (b) GI-XRD of as-deposited and annealed HZO with capping TiN electrode.

MESA structure. The annealing process for the crystallization of HZO was performed by RTA in an N_2 ambient for 30 sec.

III. RESULTS AND DISCUSSION

The Hf-based oxide is validated ferroelectricity with metal /insulator/metal structure, i.e., TiN/HZO/TiN in this work and shows the structure in Fig. 1(a). ALD is utilized for preparing HZO thin films on TiN, which is confirmed from the element composition by EDX. The thickness and lattice image of HZO are observed by HR-TEM in Fig. 1(a). To determine the phase of HZO, the GI-XRD (grazing-incident X-ray diffraction) is performed in Fig. 1(b), and crystallized HZO films after RTA with capping TiN top electrode and the polycrystalline nature are confirmed. An amorphous and crystalline structure is observed for as-deposited and annealed HZO, respectively. The crystal structure appears to be a mixture of monoclinic and tetragonal/orthorhombic/cubic phase. Note that the later three phases are difficult to distinguish due to peak positions being too close. The improvement in the FE characteristics of the HZO film after annealing at 600°C does not attribute from the increased intensity of the peaks of monoclinic phase because the ferroelectricity is believed to be a result of the formation of non-centrosymmetric orthorhombic phase [5], [8], [10].

For the ferroelectricity of HZO, we have to validate with close hysteretic loop for the polarization rather than dielectric loss due to leakage conductance of charge injection [11]. The hysteresis loops of P-E (polarization vs. E-field) show the phase transition from the as-deposited to 800°C in Fig. 2. The amorphous as-deposited HZO is a dielectric layer of capacitance with small leakage current and shows paraelectric type for a linear polarization. The polarization of crystalline HZO with 450°C and 600°C annealing exhibits FE and AFE type, respectively. With 800°C annealing, it becomes a resistance due to high leakage current along the grain boundary as shown in Fig. 4(d). Moreover, the I-V and C-V of the MFM diode are performed to validate the ferrroelectricity [12]. The current response to a triangular voltage excitation reveals the polarization switching in Fig. 3. Note that the triangular waves are used in this work for polarization extraction, due to low background conductive and capacitance current to accurately determine the spontaneous polarization [13]. Two peaks of current response for each triangular voltage peak are observed, indicating the AFE type for 600°C

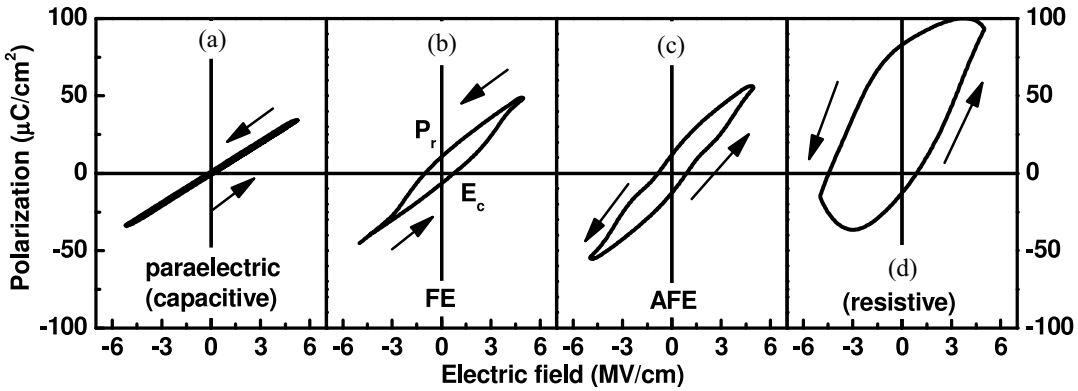

FIGURE 2. Hysteresis loops of polarization versus E-field (P-E) for HZO with (a) as-deposited, (b) 450 °C, (c) 600 °C, and (d) 800 °C. A gradual transition is observed. The amorphous HZO is a dielectric layer of capacitance and shows paraelectric type for a linear polarization. The polarization of crystalline HZO with 450 °C and 600 °C annealing exhibits FE and AFE type, respectively. With 800 °C annealing, it becomes a resistance due to high-leakage current.

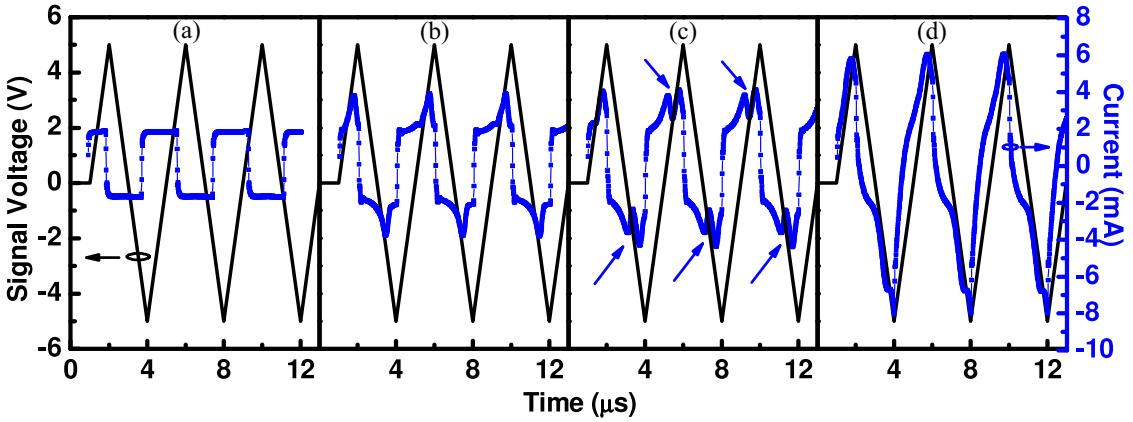

FIGURE 3. Current response to a triangular voltage for HZO with (a) as-deposited, (b) 450 °C, (c) 600 °C, and (d) 800 °C. The fast measurement of response current is done by Agilent B1530A. The current integration is to obtain polarized charge for Fig. 6. Two peaks of response current for each triangular voltage peak is observed, indicating the AFE type for annealed 600 °C HZO.

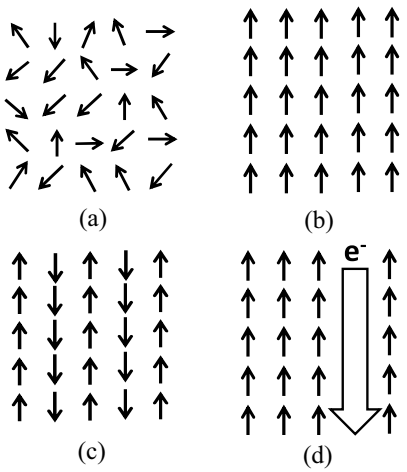

FIGURE 4. Schematic of (a) paraelectric, (b) ferroelectric, (c) antiferroelectric, and (d) ferroelectric with electrons leakage path.

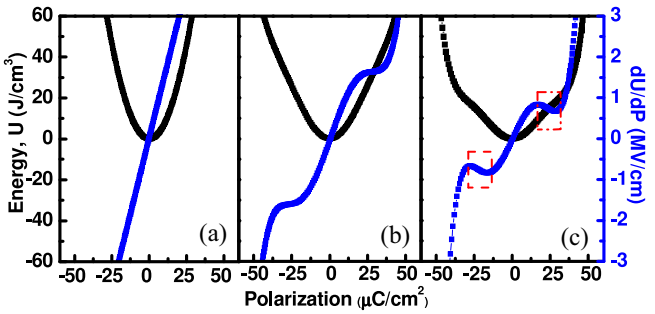

FIGURE 5. Energy landscape (*U-P*) and its derivative (*dU/dP*) of HZO with (a) as-deposited, (b) 450 °C, and (c) 600 °C. Note that the free energy is extracted from the measured P-E (Fig. 2) and based on Landau–Khalatnikov (LK) equations. The *dU/dP* of AFE HZO (600 °C) exhibits the localized negative slope and indicates existence of the NC component.

TABLE 1. Summary of the parameters in Landau–Khalatnikov (LK) equation. Note that the dielectric constant is inverse proportional to α, and $\beta = \gamma = 0$ for a ordinary linear dielectric is the as-deposited HZO.

	as dep.	450 °C (FE)	600 °C (AFE)
α (cm/F)	+7.3x10^{10}	+5.3x10^{10}	+4x10^{10}
β (cm^5/F/coul^2)	0	-2.2x10^{19}	-3.2x10^{19}
γ (cm^9/F/coul^4)	0	+5.7x10^{27}	+1.2x10^{28}

annealing HZO. The small remanent polarization (P_r), coercive field (E_c), and high dielectric constant (~ 43) of AFE type (600°C) are obtained due to reduced monoclinic phase fraction, and it is beneficial for integrated gate stacks for CMOS applications.

Gibb's free energy (*U-P*) of HZO with steady state, as shown in Fig. 5, is extracted from the measured *P-E* (Fig. 2) and based on Landau-Khalatnikov (LK) equation [14]

$$U = \alpha P^2 + \beta P^4 + \gamma P^6 - E \cdot P \quad (1)$$

$$E = 2\alpha P + 4\beta P^3 + 6\gamma P^5 \quad (2)$$

where U, P, and E are energy, polarization, and electric field, respectively. The fitting parameters of α, β, and γ are listed in Table 1. The amorphous as-deposited HZO shows a typical U-shape as the ordinary linear dielectric, and $\beta = \gamma = 0$. The dielectric constant is inversely proportional to α; therefore, the decreasing α indicates enhanced dielectric constant. The *dU/dP* of AFE HZO (600°C) exhibits the localized negative slope in Fig. 5(c) and indicates the existence of the NC component.

The steady-state surface potential (Ψ_s) is calculated according [15], [16] with the free energies.

$$V_g = (1 + a_1)\,\Psi_s + a_2\Psi_s^3 + a_3\Psi_s^5 \quad (3)$$

where $a_1 = 2\alpha C_s t_{HZO}$, $a_2 = 4\beta C_s^3 t_{HZO}$, $a_3 = 6\gamma C_s^5 t_{HZO}$. C_s, and t_{HZO} are semiconductor capacitance and HZO thickness, respectively. The non-linear behavior in surface potential of both FE and AFE HZO (450°C and 600°C) is extracted by the free energies as shown in Fig. 6(a). The surface potential gain ($d\Psi_s/dV_g$) shows more than one with voltage amplification to AFE type in Fig. 6(b).

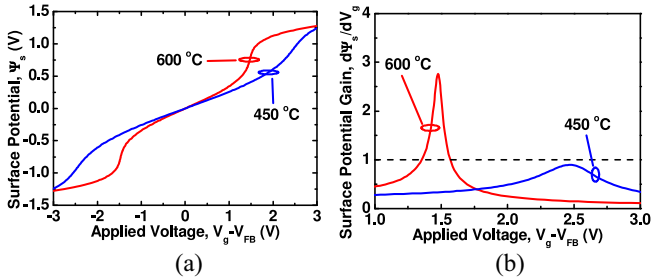

FIGURE 6. **(a) Surface potential (Ψ_s) of HZO with 450 °C and 600 °C. They are calculated [15], [16] according to the free energy and obtain the non-linear region in both FE and AFE HZO. The detailed parameters are shown in Table 1. (b) Surface potential gain ($d\Psi_s/dV_g$) of HZO with 450 °C and 600 °C. It shows more than one (2.76×) voltage amplification for AFE type. However, it is smaller than unity (0.89×) for FE.**

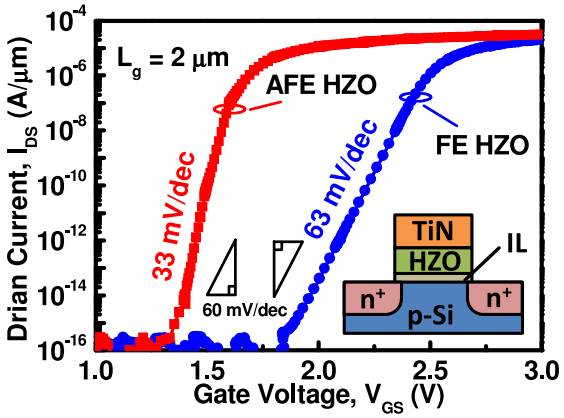

FIGURE 7. **Calculated transfer characteristics I_dV_g with the FE and AFE HZO according to Fig. 6. The subthreshold swing (SS) has been improved to 33 mV/dec for AFE HZO, but 63 mV/dec for FE HZO.**

However, it is smaller than unity for FE. This means AFE type of HZO is beneficial for NC effects by integrating FETs. The simulated transfer characteristics I_dV_g of HZO with FE and AFE to validate the surface potential gain > 1 beneficial for SS<60 mV/dec. According to the surface potential gains, it shows the steep slope (swing = 33 mV/dec) in subthreshold region for AFE (600°C) in Fig. 7. Note that the swing approximately agrees proportional to that 60 mV/dec divide to inverse of $d\Psi_s/dV_g$ (peak value of gain is around 2-3). However, there is no improvement for FE (450°C) due to $d\Psi_s/dV_g < 1$. This indicates only range ~ 0.3 V from OFF (10^{-16}A/μm) to ON (10^{-6}A/μm) state of AFE HZO MOSFET. The small turn-on operation voltage may satisfy low-power electronics application. Similar results also obtained in measurement with steep turn-on of NFET connecting AFE HZO [12]. The surface potential gain is amplified with negative capacitance effect by MFM on FET gate. This indicates that the AFE type HZO is beneficial for NC effects and CMOS application, FE HZO for memory application.

The comparison with previous studies on Hf-based oxide shows the features of the crystalline HZO with AFE type, as shown in Table 2, and exhibits electrostatic potential gain with energy landscape by ferroelectricity of HZO for low-power transistors application. The advantage of $HfZrO_x$ (Hf:Zr = 1:1) is beneficial for thickness scaling down due to cycle process of ALD with traces of dopants. The small remanent polarization and coercive field when compared with [5] and [6] is due to AFE type. A feasible concept of coupling the AFE HZO is beneficial for CMOS.

TABLE 2. **Comparison with previous studies on Hf-based oxide ferroelectricity. The AFE type are demonstrated as SS < 60 mV/dec for steep slope FET application. A feasible concept of coupling the AFE HZO is beneficial for CMOS.**

FE material	HfZrO (Hf:Zr=1:1)			other Hf-based oxide		
	this work	Ref. [5]	Ref. [6]	Si:HfO_2 [9] (Si 3.8mol%)	Y:HfO_2 [8] (Y 5.2 mol%)	Al:HfO_2 [10] (Al 7.1mol%)
Temperature	600°C	500°C	600°C	1000°C	600°C	1000°C
P_r (μC/cm²)	10	17	15	7	25	6
E_c (MV/cm)	1.2	1	1.7	0.8	1.2	0.8
Thickness (nm)	9.5	9	10	8.5	10	16.2
Type	AFE	FE	FE	FE/AFE	FE	FE/AFE

IV. CONCLUSION

The corresponding energy landscape and surface potential (Ψ_s) are deduced from the ferroelectricity of HZO, demonstrating AFE in annealed 600°C HZO with voltage amplification for calculating subthreshold swing (SS) 33 mV/dec over six decades of I_{DS}. The impact of the HZO development is compatible with the current CMOS process, as compared with conventional ferroelectric materials, such as PZT, BST, . . . etc. The advantage of $HfZrO_x$ (Hf:Zr = 1:1) is beneficial for thickness scaling down due to cycle process of ALD with traces of dopants. The fundamental physics discussion is essential and necessary for negative capacitance effect on MOSFET. The comparison with previous studies on Hf-based oxide shows the features of the crystalline HZO with AFE type, and exhibits electrostatic potential gain with energy landscape by ferroelectricity of HZO for low-power transistors application. A feasible concept of coupling the AFE HZO is experimentally established with the validity of NC and beneficial for SS-FET development in future generation.

REFERENCES

[1] G. A. Salvatore, D. Bouvet, and A. M. Ionescu, "Demonstration of subthreshold swing smaller than 60 mV/decade in Fe-FET with P(VDF-TrFE)/SiO_2 gate stack," in *IEDM Tech. Dig.*, San Francisco, CA, USA, 2008, pp. 167–170.

[2] A. Rusu, G. A. Salvatore, D. Jimenez, and A. M. Ionescu, "Metal-ferroelectric-metal-oxide-semiconductor field effect transistor with sub-60mV/decade subthreshold swing and internal voltage amplification," in *IEDM Tech. Dig.*, San Francisco, CA, USA, 2010, pp. 395–398.

[3] A. I. Khan, C. W. Yeung, C. Hu, and S. Salahuddin, "Ferroelectric negative capacitance MOSFET: Capacitance tuning & antiferroelectric operation," in *IEDM Tech. Dig.*, Washington, DC, USA, 2011, pp. 255–258.

[4] M. H. Lee *et al.*, "Ferroelectric negative capacitance hetero-tunnel field-effect-transistors with internal voltage amplification," in *IEDM Tech. Dig.*, Washington, DC, USA, 2013, pp. 104–107.

[5] J. Müller *et al.*, "Ferroelectricity in simple binary ZrO_2 and HfO_2," *NanoLetters*, vol. 12, no. 8, pp. 4318–4323, 2012.

[6] M. H. Park *et al.*, "Evolution of phases and ferroelectric properties of thin $Hf_{0.5}Zr_{0.5}O_2$ films according to the thickness and annealing temperature," *Appl. Phys. Lett.*, vol. 102, no. 24, 2013, Art. ID 242905.
[7] C. H. Cheng and A. Chin, "Low-voltage steep turn-on p-MOSFET using ferroelectric high-k gate dielectric," *IEEE Electron Device Lett.*, vol. 35, no. 2, pp. 274–276, Feb. 2014.
[8] J. Müller *et al.*, "Ferroelectricity in yttrium-doped hafnium oxide," *J. Appl. Phys.*, vol. 110, Dec. 2011, Art. ID 114113.
[9] T. S. Böscke, J. Müller, D. Bräuhaus, U. Schröder, and U. Böttger, "Ferroelectricity in hafnium oxide: CMOS compatible ferroelectric field effect transistors" in *IEDM Tech. Dig*., Washington, DC, USA, 2011, pp. 547–550.
[10] S. Mueller *et al.*, "Incipient ferroelectricity in Al-doped HfO_2 thin films," *Adv. Func. Mater.*, vol. 22, no. 11, pp. 2412–2417, 2012.
[11] J. F. Scott, "Ferroelectrics go bananas," *J. Phys. Condens. Matter*, vol. 20, no. 2, 2008, Art. ID 021001.
[12] M. H. Lee *et al.*, "Steep slope and near non-hysteresis of FET with antiferroelectric $HfZrO_2$ for low power electronics," *IEEE Electron Device Lett.*, vol. 36, no. 4, pp. 294–296, Apr. 2015.
[13] K. Miyasato, S. Abe, H. Takezoe, A. Fukuda, and E. Kuze, "Direct method with triangular waves for measuring spontaneous polarization in ferroelectric liquid crystals," *Jpn. J. Appl. Phys.*, vol. 22, no. 10, pp. L661–L663, 1983.
[14] T. Mitsui, I. Tatsuzaki, and E. Nakamura, *An Introduction to the Physics of Ferroelectrics*. London, U.K.: Gordon and Breach Science, 1976.
[15] S. Salahuddin and S. Datta, "Use of negative capacitance to provide voltage amplification for low power nanoscale devices," *NanoLetters*, vol. 8, no. 2, pp. 405–410, 2008.
[16] S. Salahuddin and S. Datta, "Can the subthreshold swing in a classical FET be lowered below 60 mV/decade?" in *IEDM Tech. Dig.*, San Francisco, CA, USA, 2008, pp. 693–696.

Authors' photographs and biographies not available at the time of publication.